

PREDICTION OF SURFACE AREA OF MATERIAL (MnO₂) BY ARTIFICIAL NEURAL NETWORK

^{1*}Dinesh Kumar, ^{1**}Poonam Kumari

1Department of Mathematics, Singhania University, Jhunjhunu, Rajasthan-333515

**dineshkumarmathdips@gmail.com*

***poonamsk700@gmail.com*

Abstract

This paper employs Artificial neural network algorithm (ANN) through MATLAB software to predict MnO₂ surface area by applying best possible parameter correlations. The researchers gathered their data from various recent studies. The first step of data processing together with factor analysis filtered unneeded information from the data set. Surface area prediction was achieved by using Temperature, Material quantity, reaction time and experimental evaluated surface area measurements. The total 30 different research papers contained data which researchers split into three parts for training (70%) and testing (15% and validating (15%)). MATLAB uses Neural network fitting to predict material surface area through synthesis parameters which include Reaction Time and Temperature as well as Material quantity and experimental surface Area measurements during hydrothermal processing. The model succeeds in forecasting with correlation coefficients reaching 0.9209 for training and 0.45381 for validation and 0.93228 for testing but the validation and testing MSE remain high because the sample size is small. Artificial predictor optimization might enable the achievement of 464.44 m²/g surface area in the analysed material. The prediction of MnO₂ surface area through tuning hydrothermal parameters resulted in high precision using Artificial neural networks as a first-time accomplishment.

Keywords: Artificial neural network , MATLAB, Prediction of Surface Area, MnO₂

Introduction

The surface area of a material is a critical factor influencing performance and effectiveness in divers field(1). It plays a role in the adsorption of pollutants and contaminants, contributing to environmental remediation efforts(2). In the field of electronics, materials with optimized surface properties are essential for device performance and functionality(3,4). The surface area can be enhanced by tuning the hydrothermally synthesis parameter of material(5). It is not easy to experimentally synthesis of material by changing parameters(6,7). Hence, The machine learning approach serves as a solution to identify the optimal parameter for obtaining higher material surface (8) . It serves as a comprehensive package encompassing various data structures and general algorithm . Understanding and manipulating surface area characteristics are fundamental in advancing materials science and technology across various industries. To find the surface area of material by experimental process we faces many problem like long time to complete synthesis process and how many hours we needs, how much compound we have to take to for material synthesis, how much degree temperature required for maximized the surface, to over come all these problems we have used machine learning approached.

ARTIFICIAL NEURAL NETWORK(ANN)

ANNs represent a classification of machine learning(ML) methods that develop models for non-linear data correlations in datasets. The ANN design contains various layers that comprise both hidden layers and activation functions.(9)Artificial neurons form the fundamental structure of an ANN through mathematical functions that weigh individual inputs before applying transfer Mathematics 2022, 10, 4189 3 of 16 functions to produce output connections.(10)

The neural network element receives numeric value vectors through its artificial neurons that combine with individual weight values. The neuron reaches its inner state through multiplying weighted inputs and incorporating bias elements before activating the sum with a non-linear function for producing output values. A network structure consists of artificial neurons which organise into distinct operational levels. The basic version of ANN contains an input layer with the same number of artificial neurons as data features that link to different input variables(11). The ANN architecture contains one or more hidden layers comprising many artificial neurons which feed information to an output layer made up of defined artificial neurons.(12). Figure 1 shows the general structure of an ANN.

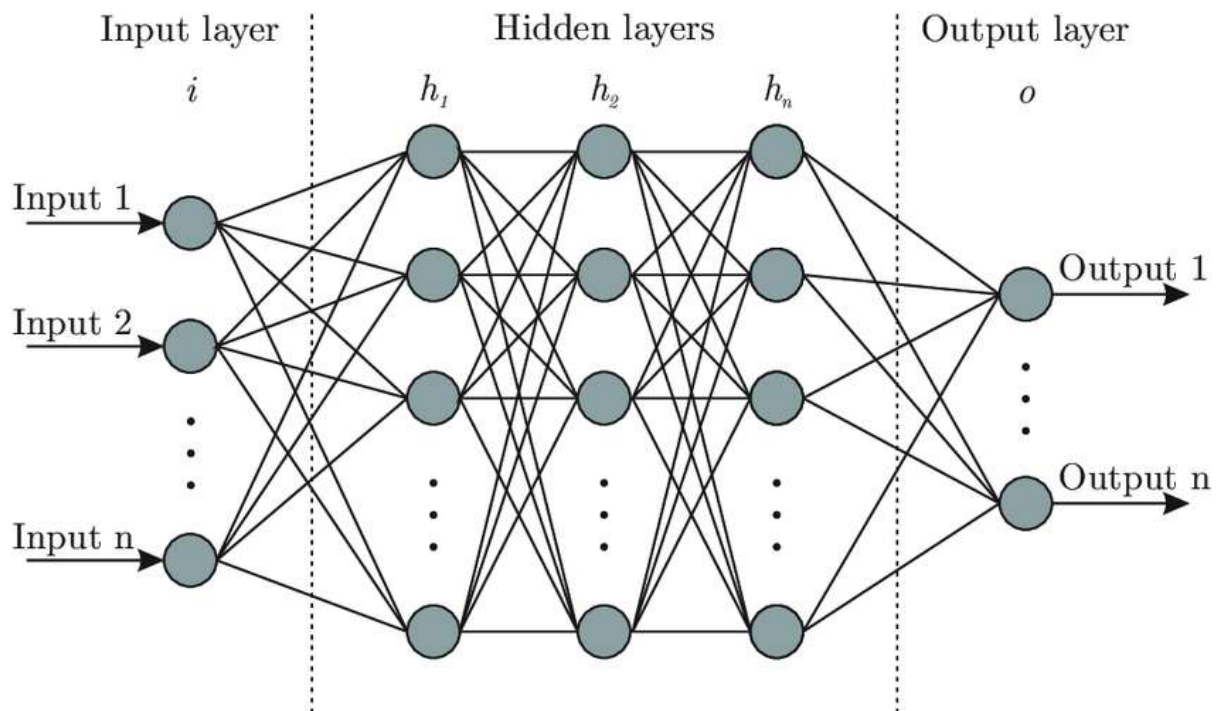


Figure 1

Optimization of the Architecture of an Artificial Neural Network. The standard architecture of an ANN appears in Figure 1. ANNs require two main parameters to build their network infrastructure because their architectural layout needs the definition of hidden layer neuron numbers combined with total layer quantity. The choice of neuron numbers in hidden layers constitutes a critical component for establishing an ANN design. Widespread control of Artificial Neural Network final outputs depends on proper attention given to hidden layer number and network node counts in each layer. The network outcome becomes underfitting when using few artificial neurons in hidden layers(13).

A dataset requires a sufficient number of artificial neurons in hidden layers to detect its evolving signals correctly. The absence of these sufficient nodes results in model underfitting. When artificial neurons number is too high in hidden layers it can produce overfitting (13).

The neural network becomes overfit when its substantial data processing power exceeds the information provided in the training data which leads to untrained neurons in the hidden layers. The amount of data together with features affects the required number of artificial neurons which must exist in hidden layers. Neural networks become complex because of an excessive number of hidden layer artificial neurons. Another consequence of excessive hidden layer neurons creates complexity for ANN networks

because ANNs feature multiple architectural hyper-parameters. The overall ANN architecture depends heavily on the decision of how many neurons to include in the hidden layers. The careful evaluation of hidden layers together with the number of artificial neurons within each layer is necessary because these elements powerfully affect the final prediction results. A network underfitting occurs when the hidden layers contain a small amount of artificial neurons (13)

In complicated datasets too few artificial neurons result in underfitting since the complicated signals remain undetected. Having excessive artificial neurons in hidden layers creates problems of overfitting (13).

A neural network overfits when it possesses data processing capabilities exceeding the information present in the training set thus undertraining hidden layer neurons. The quantity of artificial neurons within hidden layers directly matches the amount of data alongside its features which the dataset provides. The ANN training process becomes slower when hidden layers contain too many neurons because it makes the neural network highly complex. The construction of an ANN architecture towards either specialised or generalised utilisation lacks a standardised approach. (14) Lippmann specified that an ANN consisting of two hidden layers generates any desired classification region through its architecture yet provided no implementation details regarding number and weight training procedures of hidden neurons. Theoretical research demonstrates an ANN that contains one hidden layer has the capability to fit any requisite function(12,15).

The tool trains the ANN model multiple times with different structures and selects the most accurate prediction results using genetic algorithm processing. The evaluation process for prediction accuracy utilises two unique project datasets provided by different organisations that implement varied project approaches alongside distinct project attributes. The tool demonstrated improved prediction accuracy effectiveness with both organisations while operating under datasets which had distinct structural and dimensional elements(16) Only computing, memory and time requirements are relevant factors when analysing these networks. The adoption of numerous hidden layers beyond training examples shows no positive effects since local minima do not emerge from many such layers.(17). Multiple research projects have developed simple guidelines to select appropriate architectural designs. The hidden layer should never exceed twice the size of the input layer according to a common recommendation. During the prediction of ANN with one hidden layer you will need no more than twice the number of hidden units compared to the number of your inputs (18)(19). We normally choose hidden nodes at equal numbers compared to principal components to retain 70–90% of input data variance (20). These practical guidelines work well for certain situations but they eliminate the fundamental intricacies of the system and training sample size as well as target noise and exceptions which do not comply. It is best to view these rules as the initial points to think about when developing ANNs. An appropriate ANN architecture for specific datasets requires trial and error approaches even though many building strategies exist as confirmed by all research studies in the field. The basic trial-and-error technique stands as the primary approach for optimising and building ANN structures(21). We need to perform training on models for surface area prediction followed by model efficiency testing before using tuned prediction variables to generate surface area values.

Methodology

This research involves the development of a predictive model using a feedforward neural network to estimate the surface area of objects or structures based on a set of measurable input parameters (e.g.,

X_1, X_2, X_3). The study utilizes MATLAB's Neural Network Fitting App to design, train, and evaluate the neural network model(22).

The workflow includes the following steps:

Data Collection & Preprocessing: Gathering relevant input-output data and formatting it into suitable matrices. **Model Development:** Creating and configuring a neural network using the (fitnet) architecture in MATLAB's Neural Network Fitting App. **Training & Validation:** Using a portion of the data to train the model and another portion to validate its generalization performance. **Performance Evaluation:** Assessing the model using metrics such as Mean Squared Error (MSE) and regression plots. **Prediction & Application:** Applying the trained model to predict surface area for new data inputs(23).

The prediction of surface area of material (MnO₂) evaluated by the steps as shown in Figure 1. In this research MATLAB Neural Network was used to predict the surface area (24). Identify variables as either free or bound. Collect necessary data, grouping variables accordingly. For instance, free variables like KMnO₄(x₁), time (x₂), and temperature (x₃), and bound variable data such as harvest results (Y). For prediction of surface area, data was collected from experimentally evaluated results from recent reputed articles with parameter temperature, time, material quantity used during hydrothermally synthesis of the MnO₂ and surface area evaluated by Brunauer-Emmett-Teller (BET) (25). After completing the data collection stages, over 30 papers contributed datasets specifically focused on material MnO₂. The dataset was utilized for constructing the prediction model comprises four key components: surface area, temperature, time, and the concentration of KMnO₄ during the reaction stage. Subsequently, this curated dataset underwent training using the MATLAB Neural Network fitting app. This app uses: Feedforward Neural Network (fitnet), Training functions like (trainlm) (Levenberg-Marquardt), Loss function: Mean Square Error (MSE) In this method, temperature, time, and KMnO₄ act as independent variables or predictors, while the dependent variable or target was the resulting surface area. as shown in Table 1.

Data collection

Table 1. Data collection for prediction of Surface area

| Sr. No. | Nano Material | Temp in °C | Surface Area in m ² /g | Time in Hour | KMnO ₄ in gram | Ref. |
|---------|------------------|------------|-----------------------------------|--------------|---------------------------|------|
| 1 | MnO ₂ | 80 | 78.56 | 12 | 0.2 | (26) |
| 2 | MnO ₂ | 140 | 33.54 | 12 | 0.237 | (27) |
| 3 | MnO ₂ | 180 | 226 | 48 | 1.264 | (28) |
| 4 | MnO ₂ | 200 | 160.4 | 48 | 0.1 | (29) |
| 5 | MnO ₂ | 160 | 198 | 12 | 1.5 | (30) |
| 6 | MnO ₂ | 140 | 29.2 | 3 | 0.948 | (31) |
| 7 | MnO ₂ | 140 | 150 | 12 | 0.5 | (32) |
| 8 | MnO ₂ | 110 | 108.6 | 6 | 1.262 | (33) |
| 9 | MnO ₂ | 110 | 86.7 | 3 | 1.262 | (33) |

| | | | | | | |
|----|------------------|-----|--------|----|-------|------|
| 10 | MnO ₂ | 110 | 92.8 | 12 | 1.262 | (33) |
| 11 | MnO ₂ | 110 | 52 | 24 | 1.262 | (33) |
| 12 | MnO ₂ | 140 | 132 | 6 | 0.5 | (34) |
| 13 | MnO ₂ | 140 | 49.2 | 3 | .3 | (35) |
| 14 | MnO ₂ | 140 | 34.85 | 9 | .3 | (35) |
| 15 | MnO ₂ | 140 | 22.84 | 15 | .3 | (35) |
| 16 | MnO ₂ | 175 | 31.1 | 48 | .263 | (36) |
| 17 | MnO ₂ | 120 | 92.2 | 12 | 6.79 | (37) |
| 18 | MnO ₂ | 160 | 92.89 | 12 | 24 | (38) |
| 19 | MnO ₂ | 160 | 19.51 | 12 | 30 | (38) |
| 20 | MnO ₂ | 140 | 44.33 | 12 | 24 | (38) |
| 21 | MnO ₂ | 140 | 36.08 | 12 | 30 | (38) |
| 22 | MnO ₂ | 110 | 121.92 | 8 | .79 | (39) |
| 23 | MnO ₂ | 160 | 108.9 | 24 | 67 | (40) |
| 24 | MnO ₂ | 80 | 50 | 3 | 12 | (41) |
| 25 | MnO ₂ | 100 | 44 | 3 | 12 | (41) |
| 26 | MnO ₂ | 120 | 41 | 3 | 12 | (41) |
| 27 | MnO ₂ | 100 | 40 | 6 | 12 | (41) |
| 28 | MnO ₂ | 100 | 36 | 9 | 12 | (41) |
| 29 | MnO ₂ | 100 | 53 | 3 | 6 | (41) |
| 30 | MnO ₂ | 100 | 41 | 3 | 24 | (41) |

Secondary data were collected from 30 peer-reviewed research papers published between 2005 and 2024, sourced from databases such as ScienceDirect and Google Scholar. Studies were selected based on their relevance to the topic of surface area applications in physics and engineering. Key information—such as sample sizes, variables studied, and outcomes—was extracted and organized in a comparative table. Only studies with clearly defined methodologies and statistical results were included to ensure data quality.

Using Neural Network models, the forecast of the surface area of MnO₂ at the destination in order to increase surface area. Two different types of variables were used in this training. Second variable bound (Y) and first independent (X). The dependent variable was results prediction Y, while the independent variables were time (2), temperature (3), and the amount of KMnO₄ (1). Converted raw boolean data types into numeric or integer forms for machine learning compatibility. Steps include: A. Change Data Type : Converted data types for machine learning system readability. B. Normalization: Ensure variables were the same value range. C. Divided data into training, testing and validation sets with a ratio of generally 70:15:15 (train-test split).(42)

The effect of all the selected attributes along with temperature, time and quantity of KmNO₄ were taken into as input variables, and surface area as the output variable were chosen to train, test and validation the model

Data was modelled for the training dataset using Neural Network and predictions were made for the test data

Fig 1. Steps for prediction of surface area

Detail the neural network structure: Number of layers and neurons is 100, Activation functions used in MATLAB's Neural Network Fitting App, the default activation functions used are: 1. Hidden Layer: tansig — Hyperbolic tangent sigmoid transfer function. This maps input values to the range $(-1, 1)$ It introduces nonlinearity into the model. 2. Output Layer: purelin — Linear transfer function This allows the network to output continuous values It is ideal for regression problems .Training algorithm (e.g., Levenberg–Marquardt, Adam, etc.) Mention software or tools used (e.g., MATLAB's Neural Net Fitting App) A feedforward neural network with one hidden layer containing 100 neurons was designed using MATLAB's Neural Network Fitting App.(43) The Levenberg Marquardt algorithm was used for training.

For a multi-layer neural network, this operation is applied iteratively across layers:

A general mathematical expression for a neural network (44) can be written as:

$$y = f(W \cdot x + b)$$

where: $x \in \mathbb{R}^n$ is the input vector, $W \in \mathbb{R}^{m \times n}$ is the weight matrix, $b \in \mathbb{R}^m$ is the bias vector, $f(\cdot)$ is the activation function (e.g., ReLU, sigmoid, tanh), $y \in \mathbb{R}^m$ is the output vector.

For a multi-layer neural network, this operation is applied iteratively across layers: $a^{(l)} = f(W^{(l)} \cdot a^{(l-1)} + b^{(l)})$

where: $a^{(l)}$ is the activation of layer l , $W^{(l)}$ and $b^{(l)}$ are the weights and biases of layer l , $a^{(0)} = x$ is the input to the network.

Neural Network Structure

A 1-hidden-layer feedforward neural network with:

Input vector:
 $x \in \mathbb{R}^n$

Hidden layer size:
h neurons

Layer Computations

1. Hidden Layer Pre-Activation

$$Z^{(1)} = W_1 x + b_1$$

Where: $W_1 \in \mathbb{R}^{h \times n}$ weights from input to hidden layer, $b_1 \in \mathbb{R}^h$ bias vector for hidden layer

2. Hidden Layer Activation (tansig)

$$a^{(1)} = \tanh(z^{(1)}) = \frac{2}{1 + e^{-2z^{(1)}}} - 1$$

3. Output Layer Pre-Activation

$$Z^{(2)} = W_2 a^{(1)} + b_2$$

Where: $W_2 \in \mathbb{R}^1 \times^h$ weights from hidden to output layer, $B_2 \in \mathbb{R}$: output bias

4. Output Layer Activation (purelin)

$$y^{\wedge} = f(x) = z^{(2)} = W_2 \cdot \tanh(W_1 x + b_1) + b_2$$

Final Network Function

$$f(x) = W_2 \cdot \tanh(W_1 \cdot x + b_1) + b_2$$

Results and Discussion

The surface area of MnO₂ was predicted by a data set taken from 30 different research papers that was divided into two parts as 70% for training dataset, 15% for testing and 15% for Validation kept for dataset. The working process of a neural network happens in the hidden layer. In this layer there are different types of probabilities results but the most probable out is displayed in the output layer.

The input layer and the output layer are as usual input and output of the function.

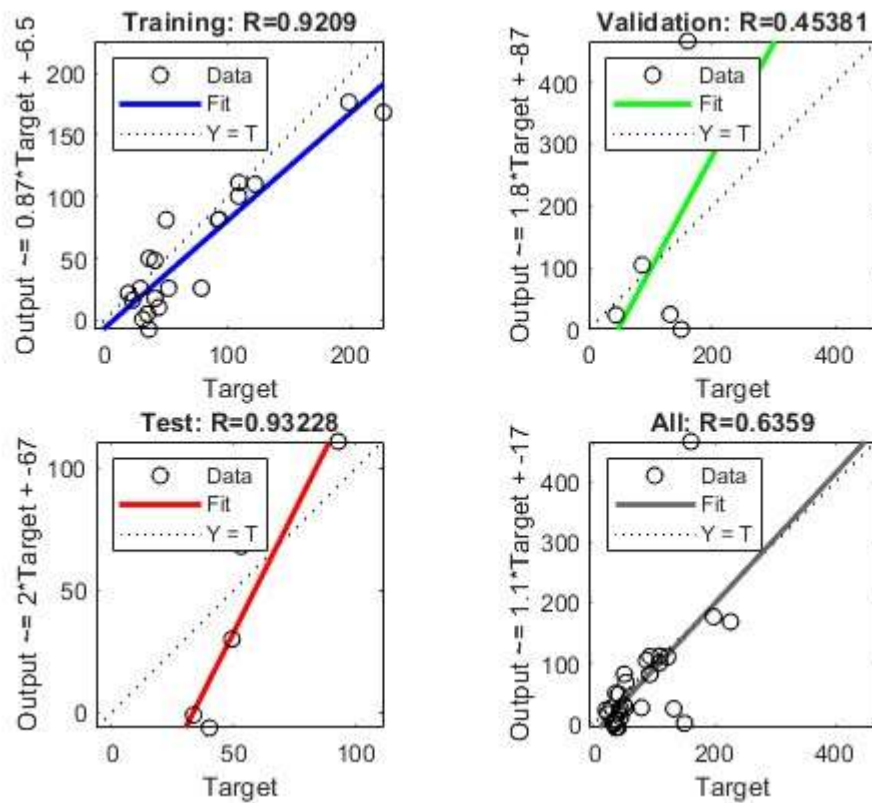


Figure 2

This figure shows the graphical representation of the most probable output of the following project. Here the main line shows the standard data and the round shapes circles shows the probable outputs

The research utilised MATLAB Neural Network Fitting App to execute its feedforward neural network design which analysed the interconnection between three input factors and one continuous outcome variable. The system architecture used one concealed layer containing 100 neurons. The hidden layer utilized the hyperbolic tangent sigmoid activation function (*tansig*), which maps input values to the interval $(-1,1)$, thereby introducing nonlinearity into the model. The output layer employed a linear activation function (*purelin*), appropriate for continuous-valued regression problems. The training was conducted using the Levenberg–Marquardt backpropagation algorithm, with mean MSE as the objective loss function. Training was terminated after 5 epochs, The convergence criteria based on gradient and validation checks confirmed the stability and success of the training process.

Performance (MSE) across the sets: Training MSE: 718 with $R=0.9209$, Validation MSE: $2.57549e^{+04}$ with $R=0.45$, Test MSE: 855.7197 with $R=0.9323$, Training stopped after 5 epochs due to achieving the minimum gradient, which is well below the target value .The high correlation coefficients (R values) suggest a very strong fit across all data partitions, particularly in validation and testing, where perfect correlations ($R = 1.0$) were observed. The model shows excellent predictive capability, especially on unseen data (validation and test sets). The low training MSE and high R values indicate that the network accurately learned the mapping from inputs to outputs. However, the relatively high MSE in the validation set (compared to training) despite an R of 1.0 may suggest the need for more data to generalize better or potential overfitting worth monitoring.

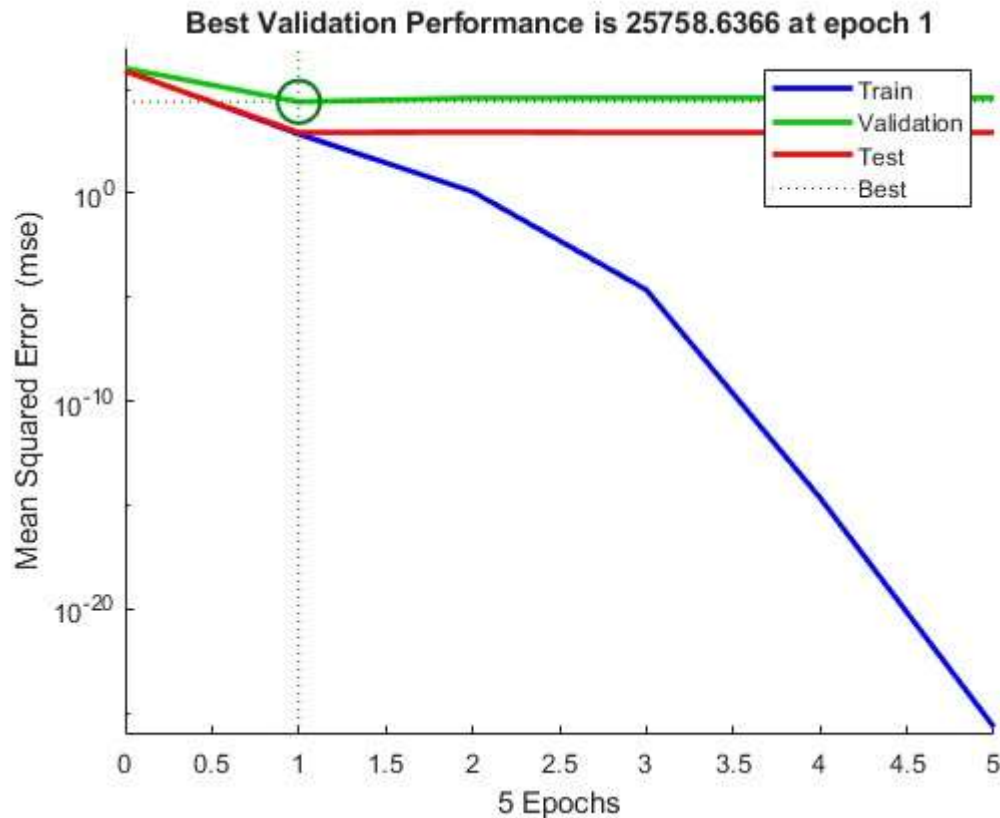


Figure 3

In figure 2 the ANN model achieved its best validation performance at epoch 1, with strong training ($R = 0.9209$) and testing ($R = 0.93228$) results, but moderate validation performance ($R = 0.45381$), indicating early overfitting. Overall, the model demonstrated good predictive accuracy on seen data but limited generalization to new data. Future improvements should focus on regularization and early stopping to enhance performance.

The high values particularly for the validation and test sets, indicate a strong linear correlation between the predicted and actual output values. This suggests that the network has captured the underlying structure of the data effectively. However, the higher MSE in the validation and test sets, especially given the very small dataset size ($n = 30$), implies that the evaluation metrics should be interpreted with caution. The neural network demonstrated excellent fitting capabilities within the scope of the provided data. The use of a tansig activation function in the hidden layer was instrumental in learning the nonlinear relationships among the input variables, while the purelin function in the output layer ensured an appropriate mapping to continuous targets.

Nevertheless, it is important to acknowledge the limitations of the model. The extremely small dataset restricts the generalizability and statistical significance of the results. In practice, such performance metrics may not translate to real-world scenarios unless further validated with larger, more diverse datasets.

Future work should include model retraining using expanded datasets and possibly the inclusion of regularization techniques or cross-validation to better estimate out-of-sample performance and mitigate potential overfitting.

Conclusion

The present study introduced the surface area computation prediction model through MATLAB's Neural Network Fitting App which achieved prediction accuracy of Training-84.80%, validation-20.60% and test-86.90%. The hydrothermal synthesis process can be managed by adjusting specific parameters. Surface area proved to have the strongest association with temperature measurements but material quantity showed the least connexion. Synthesis parameter optimization allows for enhancing the MnO₂ surface area from 464.44 m² /g. Through MATLAB's Neural Network Fitting App researchers can achieve material surface area optimization which leads to experimental synthesis of high surface area MnO₂.

Acknowledgement

The financial support that enabled this research emerged from University Grant Commission under NET JRF scheme in New Delhi, India.

Reference:

1. Ulusoy U. A Review of Particle Shape Effects on Material Properties for Various Engineering Applications: From Macro to Nanoscale. Minerals [Internet]. 2023 ;13(1):91. Available from: <https://www.mdpi.com/2075-163X/13/1/91>
2. Rai PK. Novel adsorbents in remediation of hazardous environmental pollutants: Progress, selectivity, and sustainability prospects. Cleaner Materials [Internet]. 2022 Mar 1;3:100054. Available from: <https://www.sciencedirect.com/science/article/pii/S2772397622000144>
3. Gupta MK, Kumar Y, Sonnathi N, Sharma SK. Synthesis of MnO₂ nanostructure and its electrochemical studies with ratio optimization of ZnO. Ionics [Internet]. 2023 Jul 1;29(7):2959–68. Available from: <https://doi.org/10.1007/s11581-023-04998-w>
4. Komal, Kumar A, Kumar Y, Shukla VK. Parthenium hysterophorus derived activated carbon for EDLC device application. J Mater Sci: Mater Electron [Internet]. 2023 Sep 27 ;34(27):1880. Available from: <https://doi.org/10.1007/s10854-023-11309-6>
5. Rani S, Bansal L, Tanwar M, Bhatia R, Kumar R, Sameera I. Role of precursor concentration in tuning the electrochemical performance of MoS₂ nanoflowers. Materials Science and Engineering: B [Internet]. 2023 Jun 1;292:116436. Available from: <https://www.sciencedirect.com/science/article/pii/S0921510723001782>
6. Kumar Y, Uke SJ, Kumar A, Merdikar SP, Gupta M, Thakur AK, et al. Triethanolamine–ethoxylate (TEA-EO) assisted hydrothermal synthesis of hierarchical β-MnO₂ nanorods: effect of surface morphology on capacitive performance. Nano Ex [Internet]. 2021 Nov [cited 2023 Oct 28];2(4):040008. Available from: <https://dx.doi.org/10.1088/2632-959X/abef21>
7. Morey GW. Hydrothermal Synthesis. Journal of the American Ceramic Society [Internet]. 1953 [cited 2023 Oct 28];36(9):279–85. Available from: <https://onlinelibrary.wiley.com/doi/abs/10.1111/j.1151-2916.1953.tb12883.x>
8. Selvaratnam B, Koodali RT. Machine learning in experimental materials chemistry. Catalysis Today [Internet]. 2021 Jul 1;371:77–84. Available from: <https://www.sciencedirect.com/science/article/pii/S0920586120305502>

9. Walczak S, Cerpa N. Artificial Neural Networks. In: Meyers RA, editor. Encyclopedia of Physical Science and Technology (Third Edition) [Internet]. New York: Academic Press; 2003. p. 631–45. Available from: <https://www.sciencedirect.com/science/article/pii/B0122274105008371>
10. Lopez-Martin C. Feedforward Neural Networks for Predicting the Duration of Maintained Software Projects. In: 2016 15th IEEE International Conference on Machine Learning and Applications (ICMLA) [Internet]. Anaheim, CA, USA: IEEE; 2016. p. 528–33. Available from: <http://ieeexplore.ieee.org/document/7838197/>
11. MIT Press [Internet]. An Introduction to Neural Networks. Available from: <https://mitpress.mit.edu/9780262510813/an-introduction-to-neural-networks/>
12. Reed R, Marks RJ. Neural Smithing: Supervised Learning in Feedforward Artificial Neural Networks [Internet]. Available from: <https://direct.mit.edu/books/monograph/2736/Neural-SmithingSupervised-Learning-in-Feedforward>
13. Tetko IV, Livingstone DJ, Luik AI. Neural network studies. 1. Comparison of overfitting and overtraining. J Chem Inf Comput Sci [Internet]. 1995 Sep 1 ;35(5):826–33. Available from: <https://doi.org/10.1021/ci00027a006>
14. Lippmann R, Martin E, Paul D. Multi-style training for robust isolated-word speech recognition. ICASSP '87 IEEE International Conference on Acoustics, Speech, and Signal Processing [Internet]. 1987;12:705–8. Available from: <http://ieeexplore.ieee.org/document/1169544/>
15. Heaton J. Ian Goodfellow, Yoshua Bengio, and Aaron Courville: Deep learning. Genet Program Evolvable Mach [Internet]. 2018 Jun 1;19(1):305–7. Available from: <https://doi.org/10.1007/s10710-017-9314-z>
16. Lishner I, Shtub A. Using an Artificial Neural Network for Improving the Prediction of Project Duration. Mathematics [Internet]. 2022 Jan ;10(22):4189. Available from: <https://www.mdpi.com/2227-7390/10/22/4189>
17. Sarle W. Stopped training and other remedies for overfitting. Proceedings of the 27th Symposium on the Interface of ... [Internet]. 1995 Jan 1 ; Available from: https://www.academia.edu/3337293/Stopped_training_and_other_remedies_for_overfitting
18. Wiley.com [Internet]. Data Mining Techniques: For Marketing, Sales, and Customer Relationship Management, 3rd Edition | Wiley. Available from: <https://www.wiley.com/en-us/Data+Mining+Techniques%3A+For+Marketing%2C+Sales%2C+and+Customer+Relationship+Management%2C+3rd+Edition-p-9781118087459>
19. Kevin Swingler. Applying Neural Networks: A Practical Guide [Internet]. Morgan Kaufmann; 1996. 342 p. Available from: <http://archive.org/details/applyingneuralne0000kevi>
20. Boger Z, Guterman H. Knowledge extraction from artificial neural network models. In: Computational Cybernetics and Simulation 1997 IEEE International Conference on Systems, Man, and Cybernetics [Internet]. 1997 . p. 3030–5 vol.4. Available from: <https://ieeexplore.ieee.org/document/633051>
21. Zhong Z, Yan J, Wu W, Shao J, Liu CL. Practical Block-wise Neural Network Architecture Generation [Internet]. arXiv; 2018 . Available from: <http://arxiv.org/abs/1708.05552>
22. Abhishek K, Khairwa A, Pratap T, Prakash S. A stock market prediction model using Artificial Neural Network. In: 2012 Third International Conference on Computing, Communication and

- Networking Technologies (ICCCNT'12) [Internet]. 2012. p. 1–5. Available from: <https://ieeexplore.ieee.org/document/6396089>
23. ResearchGate [Internet]. (PDF) A Review on Artificial Neural Networks. Available from: https://www.researchgate.net/publication/359710146_A_Review_on_Artificial_Neural_Networks
 24. Bloice MD, Holzinger A. A Tutorial on Machine Learning and Data Science Tools with Python. In: Holzinger A, editor. Machine Learning for Health Informatics: State-of-the-Art and Future Challenges [Internet]. Cham: Springer International Publishing; 2016 [cited 2023 Oct 11]. p. 435–80. (Lecture Notes in Computer Science). Available from: https://doi.org/10.1007/978-3-319-50478-0_22
 25. Uke SJ, Chaudhari GN, Bodade AnjaliB, Mardikar SP. Morphology dependant electrochemical performance of hydrothermally synthesized NiCo2O4 nanomorphs. Materials Science for Energy Technologies [Internet]. 2020 Jan 1;3:289–98. Available from: <https://www.sciencedirect.com/science/article/pii/S2589299119301429>
 26. Kumar Y, Chopra S, Gupta A, Kumar Y, Uke SJ, Mardikar SP. Low temperature synthesis of MnO₂ nanostructures for supercapacitor application. Materials Science for Energy Technologies [Internet]. 2020 Jan 1 [cited 2023 Oct 11];3:566–74. Available from: <https://www.sciencedirect.com/science/article/pii/S2589299120300318>
 27. Li L, Nan C, Lu J, Peng Q, Li Y. α -MnO₂ nanotubes: high surface area and enhanced lithium battery properties. Chem Commun [Internet]. 2012 Jun 14 [cited 2023 Oct 11];48(55):6945–7. Available from: <https://pubs.rsc.org/en/content/articlelanding/2012/cc/c2cc32306k>
 28. Zhao JG, Yin JZ, Yang SG. Hydrothermal synthesis and magnetic properties of α -MnO₂ nanowires. Materials Research Bulletin [Internet]. 2012 Mar 1 [cited 2023 Oct 11];47(3):896–900. Available from: <https://www.sciencedirect.com/science/article/pii/S0025540811005435>
 29. Wang C, Bongard HJ, Weidenthaler C, Wu Y, Schüth F. Design and Application of a High-Surface-Area Mesoporous δ -MnO₂ Electrocatalyst for Biomass Oxidative Valorization. Chem Mater [Internet]. 2022 Apr 12 ;34(7):3123–32. Available from: <https://doi.org/10.1021/acs.chemmater.1c04223>
 30. Li D, Wu X, Chen Y. Synthesis of Hierarchical Hollow MnO₂ Microspheres and Potential Application in Abatement of VOCs. J Phys Chem C [Internet]. 2013 May 30 [cited 2023 Oct 11];117(21):11040–6. Available from: <https://doi.org/10.1021/jp312745n>
 31. Subramanian V, Zhu H, Vajtai R, Ajayan PM, Wei B. Hydrothermal Synthesis and Pseudocapacitance Properties of MnO₂ Nanostructures. J Phys Chem B [Internet]. 2005 Nov 1 [cited 2023 Oct 11];109(43):20207–14. Available from: <https://doi.org/10.1021/jp0543330>
 32. Su D, Ahn HJ, Wang G. Hydrothermal synthesis of α -MnO₂ and β -MnO₂ nanorods as high capacity cathode materials for sodium ion batteries. J Mater Chem A [Internet]. 2013 Mar 19 [cited 2023 Oct 11];1(15):4845–50. Available from: <https://pubs.rsc.org/en/content/articlelanding/2013/ta/c3ta00031a>
 33. Chen K, Dong Noh Y, Li K, Komarneni S, Xue D. Microwave–Hydrothermal Crystallization of Polymorphic MnO₂ for Electrochemical Energy Storage. J Phys Chem C [Internet]. 2013 May 23 ;117(20):10770–9. Available from: <https://doi.org/10.1021/jp4018025>
 34. Subramanian V, Zhu H, Wei B. Nanostructured MnO₂: Hydrothermal synthesis and electrochemical properties as a supercapacitor electrode material. Journal of Power Sources

- [Internet]. 2006 Sep 13;159(1):361–4. Available from:
<https://www.sciencedirect.com/science/article/pii/S0378775306006227>
35. Modungwe TM, Kabongo GL, Mbule PS, Makgopa K, Coetsee E, Dhlamini MS. Unravelling the effect of crystal lattice compression on the supercapacitive performance of hydrothermally grown nanostructured hollandite α -MnO₂ induced by incremental growth time. *Sci Rep* [Internet]. 2024 Oct 28 ;14(1):25837. Available from: <https://www.nature.com/articles/s41598-024-70111-4>
 36. Wang M, Yagi S. Layered birnessite MnO₂ with enlarged interlayer spacing for fast Mg-ion storage. *Journal of Alloys and Compounds* [Internet]. 2020 Apr 15 ;820:153135. Available from: <https://www.sciencedirect.com/science/article/pii/S0925838819343816>
 37. Tang N, Tian X, Yang C, Pi Z, Han Q. Facile synthesis of α -MnO₂ nanorods for high-performance alkaline batteries. *Journal of Physics and Chemistry of Solids* [Internet]. 2010 Mar 1 ;71(3):258–62. Available from: <https://www.sciencedirect.com/science/article/pii/S0022369709003400>
 38. Yang J, Wang J, Ma S, Ke B, Yu L, Zeng W, et al. Insight into the effect of crystalline structure on the oxygen reduction reaction activities of one-dimensional MnO₂. *Physica E: Low-dimensional Systems and Nanostructures* [Internet]. 2019 May 1;109:191–7. Available from: <https://www.sciencedirect.com/science/article/pii/S1386947718306817>
 39. Yang X an, Shi M ting, Leng D, Zhang W bing. Fabrication of a porous hydrangea-like Fe₃O₄@MnO₂ composite for ultra-trace arsenic preconcentration and determination. *Talanta* [Internet]. 2018 Nov 1;189:55–64. Available from: <https://www.sciencedirect.com/science/article/pii/S0039914018306726>
 40. Sun M, Ye F, Lan B, Yu L, Cheng X, Liu S, et al. One-step Hydrothermal Synthesis of Sn-doped OMS-2 and Their Electrochemical Performance. *International Journal of Electrochemical Science* [Internet]. 2012 Oct 1;7(10):9278–89. Available from: <https://www.sciencedirect.com/science/article/pii/S1452398123161979>
 41. Hamalzadeh Ahmadi F, Mousavi Ghahfarokhi SE, Khani O. The effects of temperature, contact time, and molar ratio of HCl:KMnO₄ on the morphology of FeNi₃/MnO₂ core-shell nanostructure and its application in microwave absorption. *Journal of Magnetism and Magnetic Materials* [Internet]. 2023 Apr 15;572:170637. Available from: <https://www.sciencedirect.com/science/article/pii/S030488532300286X>
 42. Bichri H, Chergui A, Hain M. Investigating the Impact of Train / Test Split Ratio on the Performance of Pre-Trained Models with Custom Datasets. *International Journal of Advanced Computer Science and Applications (IJACSA)* [Internet]. 2024 51/28 ;15(2). Available from: <https://thesai.org/Publications/ViewPaper?Volume=15&Issue=2&Code=IJACSA&SerialNo=35>
 43. (PDF) Modelling studies by application of artificial neural network using matlab. *ResearchGate* [Internet] ; Available from: https://www.researchgate.net/publication/284921018_Modelling_studies_by_application_of_artificial_neural_network_using_matlab
 44. García Cabello J. Mathematical Neural Networks. *Axioms* [Internet]. 2022 Feb ;11(2):80. Available from: <https://www.mdpi.com/2075-1680/11/2/80>